

Spin glass behavior and magnetocaloric effect in amorphous alloys $\text{Ce}_2\text{Fe}_{23-x}\text{Mn}_x\text{B}_3$

Fang Wang,^{1,a)} Jun Shen,^{1,2} Jian Zhang,² Ji-rong Sun,¹ and Bao-gen Shen¹

¹State Key Laboratory of Magnetism, Institute of Physics and Centre for Condensed Matter Physics, Chinese Academy of Sciences, Beijing 100190, China

²School of Material Science and Engineering, Hebei University of Technology, Tianjin 300130, China

(Presented 12 November 2008; received 16 September 2008; accepted 20 November 2008; published online 1 April 2009)

The magnetic properties and magnetocaloric effect of amorphous alloys $\text{Ce}_2\text{Fe}_{23-x}\text{Mn}_x\text{B}_3$ ($1 \leq x \leq 6$) were investigated. The magnetic properties are sensitive to the composition. For samples with $x \leq 3$, the low fraction and isolated Fe–Mn antiferromagnetic (AFM) coupling simply align antiparallel to the majority ferromagnetic (FM) order and reduce the total magnetization but cause no noncollinearity; thus they are typical FM materials with T_C decreasing drastically from 336 to 226 K and the magnetization has a sharp drop around respective T_C without thermal hysteresis suggesting a second order phase transition resulting from their amorphous nature. For $x=4$ and 5, amorphous alloys $\text{Ce}_2\text{Fe}_{23-x}\text{Mn}_x\text{B}_3$ experience two transitions: first a paramagnetic (PM)–FM second transition at 143 and 81 K, respectively, and then a FM–spin glass (SG) transition. A PM–SG transition occurs at the freezing temperature (T_f) about 28.2 K for $x=6$. The SG behavior in amorphous alloy $\text{Ce}_2\text{Fe}_{23-x}\text{Mn}_x\text{B}_3$ can be attributed to the disordered structure resulting from their amorphous nature and the competition between the Fe–Fe FM coupling and Fe–Mn AFM negative coupling. The magnetic entropy change for alloys $\text{Ce}_2\text{Fe}_{23-x}\text{Mn}_x\text{B}_3$ with $x \leq 3$ is calculated using the Maxwell relation. © 2009 American Institute of Physics. [DOI: 10.1063/1.3072031]

Very recently soft transition metal based amorphous magnetic materials, in spite of their relatively smaller magnetic entropy change compared to that of crystalline materials, as low cost candidates for magnetic refrigerants have attracted much attention due to their special merits coming from their random atomic structure: reduced magnetic hysteresis, higher electrical resistivity, tunable Curie temperature (T_C), and their outstanding mechanical properties. Moreover, alloying compositions are easily varied raising the possibility of composite structures usable in refrigerators operating over a very wide temperature range.^{1–5}

In this paper we studied the magnetic properties and magnetocaloric effect of amorphous alloys $\text{Ce}_2\text{Fe}_{23-x}\text{Mn}_x\text{B}_3$ ($x=1–6$).

Ingots with a nominal composition of $\text{Ce}_2\text{Fe}_{23-x}\text{Mn}_x\text{B}_3$ ($x=1–6$) were prepared by arc melting the mixture of high-purity Ce, Fe, Fe–B alloy, and Mn in argon atmosphere. An excess of 10% for Mn and an excess of 5% for Ce were used due to the volatilization during the melting process. Each ingot was remelted four times to ensure the homogeneity of composition in samples, and amorphous ribbons were obtained from the ingot by means of standard melt spinning in purified argon atmosphere with wheel speed of 40 m/s. The amorphous character of the ribbons was checked by x-ray diffraction (XRD). The dc and ac magnetizations were measured using a magnetic property measurement system and a physical property measurement system. XRD performed on the ribbons reveals that the ribbons are amorphous characterized by a broad intensity maximum.

Temperature dependence of magnetization (M – T) for amorphous alloys $\text{Ce}_2\text{Fe}_{23-x}\text{Mn}_x\text{B}_3$ ($x=1–6$) under a field of 0.01 T is shown in Fig. 1, and both the M – T curves of zero-field-cooled (ZFC) and field-cooled (FC) modes for $x=5$ and 6 were given. Amorphous alloys $\text{Ce}_2\text{Fe}_{23-x}\text{Mn}_x\text{B}_3$ with $x \leq 3$ are typical ferromagnetic materials with T_C decreasing drastically and almost linearly from 336 to 226 K with x varying from 1 to 3 and the magnetization has a sharp drop around respective T_C without thermal hysteresis suggesting a second order phase transition resulting from their amorphous nature. For $x=4$ and 5, amorphous alloys $\text{Ce}_2\text{Fe}_{23-x}\text{Mn}_x\text{B}_3$ experience two transitions: first a PM–FM second transition at 143 and 81 K, respectively, and then a FM–SG transition [re-entrant SG (RSG) transition]. A PM–SG transition occurs at the freezing temperature T_f of about 28.2 K for $x=6$ with

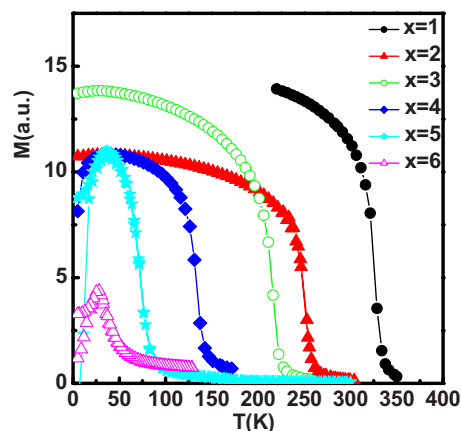


FIG. 1. (Color online) Temperature dependence of magnetization M – T curve at 0.01 T for amorphous alloys $\text{Ce}_2\text{Fe}_{23-x}\text{Mn}_x\text{B}_3$ ($x=1–6$). Both ZFC and FC M – T curves were shown for the sample with $x=5$ and 6.

^{a)}Electronic mail: wangfang@g203.iphy.ac.cn.

an obvious divergence between the ZFC and FC curves below T_f .⁷

Figure 2(a) shows the isothermal field dependent magnetization (M - H) curves of amorphous alloys $Ce_2Fe_{23-x}Mn_xB_3$ ($x=1-6$) at 5 K. For the samples with $1 \leq x \leq 4$, they show typical ferromagnetic behavior. While for the samples with $x=5$ and $x=6$, it is hard to saturate even at the applied field of 5 T, which is a typical characteristic of SG system. The saturated magnetization M_s decreases linearly from 129 to 26 emu/g. If Fe moment is assumed to be unchanged as $1.8\mu_B$ by the Mn substitution, we can deduce that Mn atoms couple antiparallel to Fe with the magnetic moment of $-3.4\mu_B$. Due to the antiferromagnetic (AFM) coupling between Fe and Mn atoms, the magnetization of amorphous alloys $Ce_2Fe_{23-x}Mn_xB_3$ ($x=1-6$) is sensitive to a slight change in composition. M_s decreases significantly linearly with Mn concentration x as displayed in Fig. 2(b).

To verify the SG state in the amorphous alloy $Ce_2Fe_{17}Mn_6B_3$, the T -dependent ac susceptibility $\chi(T)$ is measured at several frequencies ω ranging from 10 Hz to 10 kHz as shown in Fig. 3. The $\chi'(T)$ curve displays a peak at the SG transition temperature $T_f(\omega)$, which is frequency dependent. The peak temperature $T_f(\omega)$ shifts toward higher temperatures and the height of the susceptibility peak dimin-

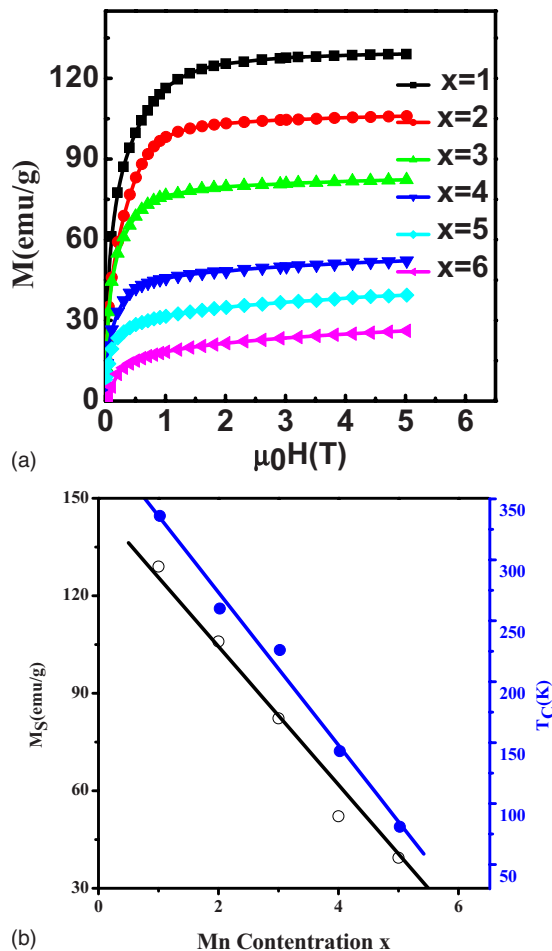


FIG. 2. (Color online) (a) The isothermal field dependent magnetization (M - H) curves of amorphous alloys $Ce_2Fe_{23-x}Mn_xB_3$ ($x=1-6$) at 5 K. (b) Mn concentration x dependences of the Curie temperature (T_C) and the saturated magnetization (M_s).

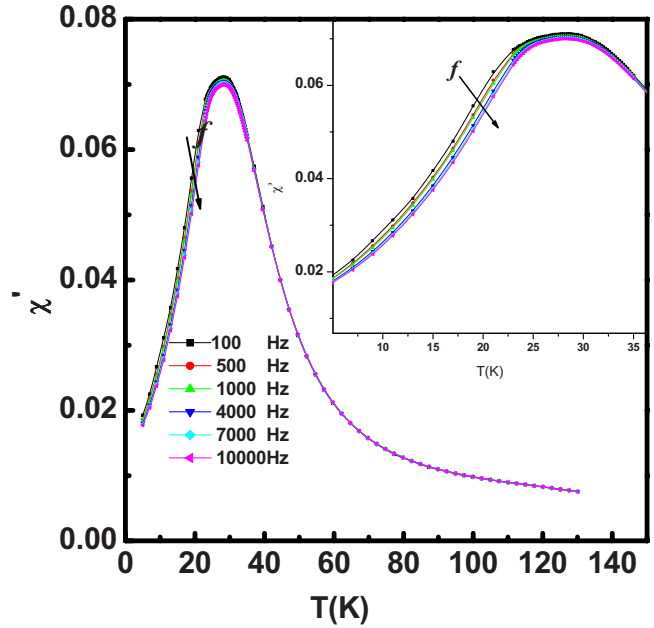


FIG. 3. (Color online) The T -dependent ac susceptibility $\chi(T)$ at several frequencies ω ranging from 10 Hz to 10 kHz.

ishes with increasing frequency. The value of the frequency sensitivity of $T_f(\omega)$, $\Delta T_f(\omega) / [T_f(\omega) \Delta \log_{10} \omega]$, which has been used as a possible distinguishing criterion for the presence of a spin-glass phase, is 0.007, very close to that of the conventional spin glasses.⁸

The M - H loop at 5 K of amorphous alloy $Ce_2Fe_{17}Mn_6B_3$ is shown in Fig. 4. From the inset amplificatory graph around the coercive force, one can see that there is a displacement in the loop. Furthermore, the initial magnetization curves are different from that of the typical ferromagnetic materials; the magnetization increases slowly in the low applied field and increases rapidly after the applied field larger than 1000 G, as shown in the inset of Fig. 4.

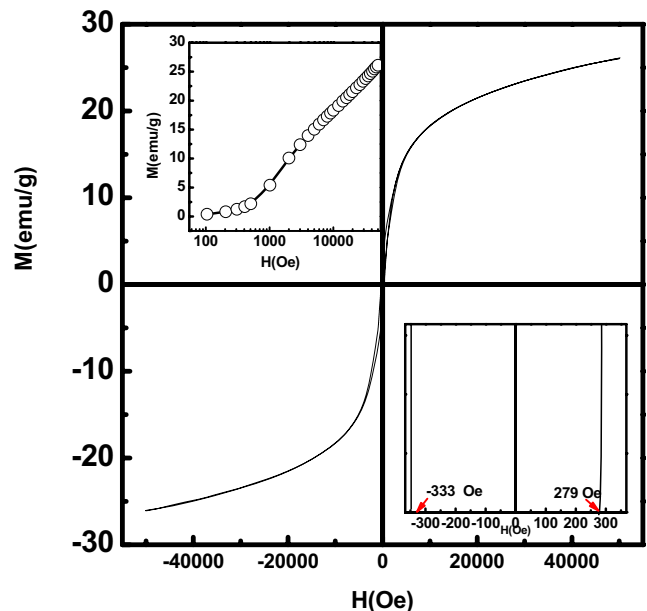


FIG. 4. (Color online) The M - H loop at 5 K of amorphous alloy $Ce_2Fe_{17}Mn_6B_3$. The inset shows the initial magnetization curves at 5 K with logarithm label.

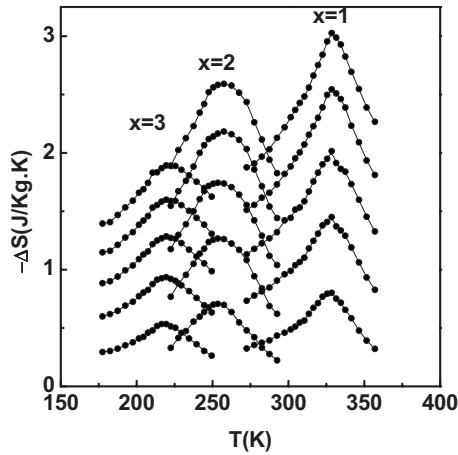


FIG. 5. The temperature dependent magnetic entropy change in the different applied field changes for the samples with $x=1, 2$, and 3 .

The SG behavior in amorphous alloy $\text{Ce}_2\text{Fe}_{23-x}\text{Mn}_x\text{B}_3$ can be attributed to the disordered structure resulting from their amorphous nature and the competition between the Fe–Fe FM coupling and Fe–Mn AFM negative coupling. It can only be induced for a sufficiently high Mn concentration. The low fraction and isolated Fe–Mn AFM coupling simply align antiparallel to the majority FM order and reduce the total magnetization but cause no noncollinearity. The frustration only appears when the Mn concentration is high enough for AFM-AFM pairs to occur; first RSG appears and then SG appears with further increasing Mn concentration.

Although the structure is disordered due to the fact that it is amorphous, the magnetization has a sharp drop around T_C for amorphous alloys $\text{Ce}_2\text{Fe}_{23-x}\text{Mn}_x\text{B}_3$ ($x=1, 2$, and 3). According to the Maxwell relation, the sharp drop of magnetization around T_C indicates a large magnetic entropy change for these amorphous alloys. The field-dependent isothermal magnetization curves M - H in a wide temperature range around T_C were measured. A temperature step of 3 K was adopted in the vicinity of T_C and that of 5 K for the far regions. The nonlinear behavior of M - H curve above T_C may be caused by the partially crystalline phase corresponding to $\text{Ce}_2(\text{Fe}, \text{Mn})_{23}\text{B}_3$ crystalline compound with higher T_C than that of amorphous alloys. Compared to the surface of the ribbon that was on contact with the wheel, the volume of the ribbons, which was frozen more slowly, is partially crystallized. However, no obvious sharp peak patterns, characteristic of crystalline phase, are observed in the XRD of powder samples probably due to the slight fraction of crystalline phase.

The magnetic entropy change ΔS_M is calculated from the isothermal magnetization by the Maxwell relation,

$$\Delta S_M(T, H) = \int_0^H \left(\frac{\partial M}{\partial T} \right)_H dH,$$

where ΔS_M , T , H , and M are the magnetic entropy, temperature, applied magnetic field, and magnetization of the material, respectively.⁹ Figure 5 shows the temperature dependent magnetic entropy change in the different applied field changes. One can see that T_C decreases with increasing Mn concentration; thus the position of the maximum of ΔS_M

shifts to low temperature from above room temperature, 326–226 K, and the maximum value of ΔS_M also decreases from 3 to 2 J/kg K for a field change of 0–5 T with x increasing from 1 to 3 due to the decrease in magnetization. Although the maximum of ΔS_M is smaller than those of many crystal materials, a very broad distribution of ΔS_M is achieved, and its shape is much more uniform which is desirable for an Ericson-cycle magnetic refrigerator. Since the high temperature refrigeration implies a wider temperature range than that of the low temperature refrigeration, the RC is employed in order to compare the performance of different materials. In this paper the method suggested by Wood and Potter⁶ was used, where the RC is defined as the area of $\text{RC} = \Delta S \Delta T$, where ΔS is the magnetic entropy change at the hot and cold ends of the cycle and ΔT is a temperature span $\Delta T = T_h - T_c$. Here, values for T_h and T_c are defined by the full width at half maximum of the $\Delta S_M - T$ curve. The value of RC for amorphous alloy $\text{Ce}_2\text{Fe}_{22}\text{MnB}_3$ is found about 225 J/kg for a magnetic field change of 0–5 T, in spite of their relatively small magnetic entropy change, which is comparable to that of the best crystalline material with T_C around room temperature, such as $\text{Gd}_5\text{Ge}_2\text{Si}_2$ (200 J/kg), $\text{Gd}_5\text{Ge}_{19}\text{Si}_2\text{Fe}_{0.1}$ (235 J/kg),¹⁰ and $\text{MnFeP}_{0.45}\text{As}_{0.35}$ (225 J/kg).⁴ Furthermore the cost is reduced significantly due to the high concentration of low cost transition metals, Fe and Mn. Combining their special merits coming from the amorphous nature, the amorphous alloys $\text{Ce}_2(\text{Fe}_{1-x}\text{Mn}_x)_{23}\text{B}_3$ are a good magnetic refrigerant in a wide temperature range from 226 K to above room temperature, 336 K.

In conclusion, magnetic properties and magnetocaloric effect of amorphous alloys $\text{Ce}_2\text{Fe}_{23-x}\text{Mn}_x\text{B}_3$ ($x=1-6$) were studied. The magnetic state is sensitive to the composition x . A PM-FM transition occurs at the respective T_C for $x \leq 3$, with increasing Mn concentration; a SG behavior at low temperature was observed with Mn concentration exceeding 4. Furthermore, amorphous alloy $\text{Ce}_2\text{Fe}_{23-x}\text{Mn}_x\text{B}_3$ ($x=1, 2$, and 3) is a material with second order phase transition and the magnetic entropy change was calculated using the Maxwell relation

This work was supported by the National Basic Research Program of China, the Basic Research Program of Chinese Academy of Science, and the Knowledge Innovation Project of the Chinese Academy of Sciences.

¹N. Q. Hoa, D. T. H. Gam, N. Chau, and S. C. Yu, *J. Magn. Magn. Mater.* **310**, 2483 (2007).

²S. G. Min, K. S. Kim, S. C. Yu, H. S. Suh, and S. W. Lee, *J. Appl. Phys.* **97**, 10M310 (2005).

³V. Franco, C. F. Conde, J. S. Blázquez, and A. Conde, *J. Appl. Phys.* **101**, 093903 (2007).

⁴F. Johnson and R. D. Shullb, *J. Appl. Phys.* **99**, 08K909 (2006).

⁵Tadashi Mizoguchi, Supplement to Science Representative TITU, 1978 (unpublished), p. 117.

⁶M. E. Wood and W. H. Potter, *Cryogenics* **25**, 667 (1985).

⁷Joonghoe Dho, W. S. Kim, and N. H. Hur, *Phys. Rev. Lett.* **89**, 027202 (2002).

⁸J. A. Mydosh, *Spin Glasses: An Experimental Introduction* (Burgess, London, 1993), p. 68.

⁹V. K. Pecharsky and K. A. Gschneidner, Jr., *J. Magn. Magn. Mater.* **200**, 44 (1999).

¹⁰V. Provenzano, A. Shapiro, and R. D. Shull, *Nature (London)* **429**, 853 (2004).